THYROID
Volume 25, Number 1, 2015

DOI: 10.1089/thy.2014.0119

New Small Molecule Agonists to the Thyrotropin Receptor

Rauf Latif,[1] M. Rejwan Ali,[1] Risheng Ma,[1] Martine David,[1] Syed A. Morshed,[1]
Michael Ohlmeyer,[2] Dan P. Felsenfeld,[3] Zerlina Lau,[3] Mihaly Mezei,[2] and Terry F. Davies[1]

Background: Novel small molecular ligands (SMLs) to the thyrotropin receptor (TSHR) have potential as improved molecular probes and as therapeutic agents for the treatment of thyroid dysfunction and thyroid cancer.
Methods: To identify novel SMLs to the TSHR, we developed a transcription-based luciferase-cAMP high-throughput screening system and we screened 48,224 compounds from a 100K library in duplicate.
Results: We obtained 62 hits using the cut-off criteria of the mean ± three standard deviations above the baseline. Twenty molecules with the greatest activity were rescreened against the parent CHO-luciferase cell for nonspecific activation, and we selected two molecules (MS437 and MS438) with the highest potency for further study. These lead molecules demonstrated no detectible cross-reactivity with homologous receptors when tested against luteinizing hormone (LH)/human chorionic gonadotropin receptor and follicle stimulating hormone receptor–expressing cells. Molecule MS437 had a TSHR-stimulating potency with an EC_{50} of 13×10^{-8} M, and molecule MS438 had an EC_{50} of 5.3×10^{-8} M. The ability of these small molecule agonists to bind to the transmembrane domain of the receptor and initiate signal transduction was suggested by their activation of a chimeric receptor consisting of an LHR ectodomain and a TSHR transmembrane. Molecular modeling demonstrated that these molecules bound to residues S505 and E506 for MS438 and T501 for MS437 in the intrahelical region of transmembrane helix 3. We also examined the G protein activating ability of these molecules using CHO cells co-expressing TSHRs transfected with luciferase reporter vectors in order to measure $G_{s\alpha}$, $G_{\beta\gamma}$, $G_{\alpha q}$, and $G_{\alpha 12}$ activation quantitatively. The MS437 and MS438 molecules showed potent activation of $G_{s\alpha}$, $G_{\alpha q}$, and $G_{\alpha 12}$ similar to TSH, but neither the small molecule agonists nor TSH showed activation of the $G_{\beta\gamma}$ pathway. The small molecules MS437 and MS438 also showed upregulation of thyroglobulin (*Tg*), sodium iodine symporter (*NIS*), and *TSHR* gene expression.
Conclusions: Pharmacokinetic analysis of MS437 and MS438 indicated their pharmacotherapeutic potential, and their intraperitoneal administration to normal female mice resulted in significantly increased serum thyroxine levels, which could be maintained by repeated treatments. These molecules can therefore serve as lead molecules for further development of powerful TSH agonists.

Introduction

Small molecular ligands (SMLs) to G protein coupled receptors (GPCRs), both agonists and antagonists, have great potential as therapeutic agents because of three important characteristics: (a) SMLs can cross cell membranes easily and rapidly, (b) SMLs can be administered orally, and (c) SMLs can be synthesized at low cost. For these reasons, there is a significant effort in identifying novel small molecules that target the thyrotropin receptor (TSHR) because of their potential use in the treatment of patients with thyroid dysfunction and in the management of differentiated thyroid cancer (1,2).

Thyrotropin (TSH) is a heterodimeric glycoprotein hormone secreted from the anterior pituitary and mediates its action through the TSHR, which is a member of the class A GPCR family. The holoreceptor consists of 764 amino acids divided into three regions. The first is a large, highly glycosylated ectodomain of which the initial 260 amino acids incorporate 10 leucine-rich repeats and which has been crystallized bound to a stimulating TSHR antibody (3). The second part of the ectodomain is a region of 130 amino acids

[1]Thyroid Research Unit, Department of Medicine, Icahn School of Medicine at Mount Sinai and the James J. Peters VA Medical Center, New York, New York.
[2]Department of Structural and Chemical Biology, Icahn School of Medicine at Mount Sinai, New York, New York.
[3]Integrated Screening Core, Experimental Therapeutics Institute, Icahn School of Medicine at Mount Sinai, New York, New York.

and is known as the signal-specific domain (SSD) or ''hinge region'' (4–6) incorporating two additional leucine-rich repeats and a unique 50 amino acid insert. A partial homology model of this enigmatic hinge connecting the ectodomain to the third part of the receptor—the transmembrane domain (TMD)—has been derived from the recently crystallized follicle stimulating hormone (FSH) receptor hinge region (7). The TMD consists of 349 amino acids typical of the GPCR class A family incorporating seven transmembrane helices (TMH) joined by extracellular (ECL) and intracellular (ICL) loops (8).

The TSHR is primarily expressed in the thyroid to carry out its physiologic role in thyroid cell growth and hormone synthesis/secretion, but it also happens to be a primary autoantigen in autoimmune thyroid disease, especially Graves' disease (8–10). In addition to its primary site on the thyroid cell, the TSHR is expressed in a variety of extrathyroidal tissues where it is known to modulate target cell function (9). For example, the roles of the TSHR in Graves' orbitopathy, adipogenesis, and bone metabolism have been extensively studied (11–13). Therefore, modulating the function of the receptor either orthosterically using monoclonal antibodies (14) or allosterically, in either a positive or negative fashion, using SMLs (15–17) has therapeutic potential. Investigations by Neumann *et al*. using chemical modification of reported SML agonists of the luteinizing hormone/chorionic gonadotropin receptor (LH/hCGR) (18) have resulted in small molecule agonists and antagonists to the TSHR in the nanomolar range (15,16), while other reports of potent small molecular antagonists to the TSHR lacked receptor specificity (19). Thus, there remains a need to develop higher potency small molecule agonists and antagonists to the TSHR to develop into therapeutic drugs.

Molecular modeling studies have provided considerable insight into the mode of action of these small molecule agonists (20). SMLs by virtue of their small size can permeate the cell and dock with polar and nonpolar residues in the TMD region and exert their effects in an allosteric manner (21). In the case of the TSHR, the different transmembrane helices and intracellular and extracellular loops connecting these helices have been studied extensively for activating and inactivating mutations (22), which are the ''hot-spots'' in the receptor, having been found in human pathological conditions (21). Based on such modeling and mutational analysis of TSHR ''hot-spots,'' there appear to be two clusters of residues spanning the TM helices that are preferred mutation sites, as well as potential sites for docking of selected small molecules (20,23). Perturbations in and around the vicinity of these ''hot-spots'' are thought to lead to conformational changes in the intrahelical regions, which can either distort the basal constrained structure of these helices (24) or/and disrupt a polar interaction between a partially conserved motif on the end of TM3 and another conserved polar reside at the base of TM6, leading to disruption or destabilization of the ''ionic lock'' as seen in most GPCRs, including the TSHR (25–27).

In this report, we describe the identification and characterization of two new potent and novel small molecule agonists to the TSHR selected using a luciferase based high-throughput screening (HTS) assay. The ability of these lead molecules to activate different G proteins has been studied in addition to their pharmokinetic (PK) characteristics and their ability to cause the release of thyroxine (T4) in treated animals.

Materials and Methods

Materials

Bovine TSH (1 IU/mL), human FSH (70 IU/mL), human chorionic gonadotropin (hCG) (10 IU/vial), and forskolin were purchased from Sigma-Aldrich (St. Louis, MO). The Bright-Glo^{TM} luciferase substrate (Cat # E2610) was purchased from Promega Corp. (Madison, WI). The cell culture medium Dulbecco's modified Eagle's medium (DMEM) and Ham's F12 were purchased from Mediatech, Inc. (Manassas, VA). Fetal bovine serum (FBS) and fetal calf serum were purchased from Atlanta Biologicals (Flowery Branch, GA). Additional amounts of the lead compounds that we have identified in our screen were purchased from ChemBridge Corp. (San Diego, CA). Mouse primary Sertoli cells were obtained from ATCC (Manassas, VA). The L1 library, a collection of 100,000 molecules from Chembridge that satisfy most of the Lipinski's Rule of Five, was obtained from the Integrated Screening Core at the Icahn School of Medicine at Mount Sinai, New York.

Stable cell lines used

CHO-HA-TSHR luciferase cells. For HTS, we used cells generated by transfecting the pGL4.29 [luc2P/CRE/Hygro] construct into a highly selected stable line of CHO cells expressing the human TSHR with a HA (hemagglutinin) tag at the N-terminus (CHO-HA-TSHR cells) that has been previously described (28) and selected as a stable line with hygromycin.

TSHR/LHR chimeric luciferase cells. We used a construct pSV2-neo-ECD-TSH-LHR-11 (kindly provided by Dr. Basil Rapoport, Cedars-Sinai Research Institute and University of California, Los Angeles, CA), where a 367 amino acid insert containing the homologous regions of the rat LH/hCGR sequence replaced the TSHR ectodomain (29), which was then co-transfected with the pGL4.29 [luc2P/CRE/Hygro] construct in CHO cells and further selected for double transfectants.

CHO luciferase cells. These cells were generated by transfecting the pGL4.29 [luc2P/CRE/Hygro] construct into the CHO PSVL cells (JPO2) and selecting with hygromycin for stable transformants. The best stable clone was selected based on different concentrations of forskolin and unresponsiveness to TSH.

Each of these stable cell lines were cultured in Ham's F12 medium with 10% FBS, 100 IU/mL of penicillin, 100 μg/mL of streptomycin, and 50 μg/mL of hygromycin.

Primary Sertoli cells (line TM4). These FSHR-expressing cells were obtained from ATCC (CRL-1715) and cultured in DMEM: F12 medium (cat # 30-2006) with 2.5% FBS and 5% horse serum (ATCC; cat #30-2040).

LHR-expressing cells. The specificity against the LH/hCGR was tested using a stable line of rat hCGR in HEK 293

cells that we obtained from Dr. K.M.J. Menon (University of Michigan, Ann Arbor, MI).

Stable lines of luciferase constructs for G protein activation. For signaling studies of various G proteins, we used cells generated as previously described (30). We used double-transfected stable lines of CHO-HA-TSHR with pGL4.34 [luc2P/SRF-RE/Hygro] to detect $G_{\alpha 12}$, pGL4.33[luc2P/SRE/Hygro] to detect $G_{\beta\gamma}$, and pGL4.30 [luc2P/NFAT-RE/Hygro] to detect $G_{\alpha q}$. These double-transfected stable lines were also maintained in complete Ham' F12 medium with appropriate concentrations of hygromycin.

HTS luciferase assay

To develop the screening assay, a high expressing stable line of CHO-HA-TSHR cells carrying an amino terminus HA tagged TSHR was selected. This stable CHO line was transfected with the construct pGL4.29 [CRE/minP/luc2P] carrying a minimal promoter driving a CREB response element (CRE) tagged to a modified form of the luciferase reporter gene *luc2P* (Promega Corp.). *Luc2P* is a modified firefly luciferase sequence with humanized codon optimization that is designed for high expression and reduced anomalous transcription. In addition, the *luc2P* gene contains hPEST, a protein destabilization sequence, which further reduces background transcribed protein (31). Activation of the TSHR by TSH or an agonist results in $G_{s\alpha}$-adenylate cyclase coupling and an increase in intracellular cAMP, which results in the activation of CREB at its binding to the CRE element and subsequently in the transcription of the *luciferase* gene and accumulation of the luciferase enzyme within the activated cells. Luciferase activity in these cells was detected after lysing the cells using the commercial substrate Bright-Glo™. For HTS, we seeded 15,000 cells of transfected CHO-HA-TSHR cells per well in a 384 opaque white-bottom poxi-plate (ProxiPlate cat # 6008230; PerkinElmer, Branford, CT) using a Multidrop Combi dispenser (Thermo Fisher, Waltham, MA) in 10 μL of Ham's F12 complete medium, and incubated overnight at 37°C in a CO_2 incubator with a relative humidity of >85%. Small molecule libraries were added from 384-well stock plates containing 10 mM solutions in DMSO (Chembridge Corp.). Small molecule addition was accomplished using a 384-tip pin tool (V&P Scientific, San Diego, CA) transferring 17 nL per pin (based on fluorimetric calibration), resulting in a final concentration of 17 μM per well. Plate validation and normalization controls, including negative control (medium only) with 0.1% DMSO and a positive agonist molecule previously described (15), were added to blank wells located in the first two and last two columns of each plate. Following compound addition, plates were incubated for 4 h at 37°C. After 4 h, the cells were lysed by adding 6 μL of Bright-Glo™ reagent, and incubated for 2 min before measuring luciferase activity using an EnVision Multilabel Plate Reader (PerkinElmer). Throughout the screen of 137 plates, the signal-to-background ratio was linear, the mean CV was 12%, and the Z′ factor was in the range 0.7–0.8 based on the positive control used in the plate, which exceeds the commonly accepted threshold (0.5) for validation of high-throughput assays (32). Dose–response relationships of the lead molecules were determined using a Tecan HP dispenser by following a similar protocol. Data points of the dose–response curves were fitted using Prism 5.0.

Docking of lead molecules on the TSHR transmembrane

Docking of the lead molecules was performed on a homology model of the TSHR-TMD based on rhodopsin (PDB:1F88). This template was chosen because of the low RMSD values between the backbone of the TM helices of the TSHR model and that of the rhodopsin x-ray crystal structure (33), and fits the experimental parameters previously described (34). The initial homology model of rhodopsin was obtained from the Uniprot server (www.uniprot.org). The conformations of the extracellular loops were constructed with the Monte Carlo method (35). Prior to docking, an *ab initio* geometry optimization of the lead molecules was carried out with the Gaussian 09 program using the HF/6-31G* basis implementing a tight binding self-consistent field (36). The 3D geometries of the molecules in mol2 format were obtained from the Gaussian output using AMBER Antechamber tools (37,38). The binding sites of the lead molecules were obtained using a grid-box enclosing the entire physiological receptor target region, including the seven helices and three extra cellular loops. The orientation of the receptor was optimized using Simulaid (39) to facilitate the docking grid; docking was carried out using the docking suits eHiTS, Autodock 4, and Vina. The docking results were analyzed using DOCKRES and other supporting scripts tools (40).

Molecular dynamics simulation of lead molecules

To assess the quality of the binding pocket further, we performed a 10 ns full-scale molecular dynamics simulation of bound poses of the lead molecules using the AMBER software suite v12 that uses force field 12SB (41). The initial docked conformation as analyzed for binding sites was obtained by DOCKRES (40). All the force field parameters of the two lead compounds interacting via only nonbonded parameters with the receptor were obtained by Antechamber tools using Gaussian calculations. The topology and initial coordinates of the lead molecules forming complexes with TSH-TMD were created with the AMBER LEAP module (41).

Molecular dynamics on both complexes was carried out under periodic boundary conditions (PBC) with 10 Å nonbonded cutoff lengths. A total of 1000 minimization steps composed of 500 conjugate gradient and 500 steepest descent were performed followed by the heating cycles. The first heating cycle of 5000 steps was followed by a heating cycle of 50,000 steps that equilibrated the system temperature to a simulation temperature of 300 K. The final MD simulation of the complexes at constant pressure and temperature were carried out for 10 ns with a 2 fs integration step size. The trajectories were analyzed and visualized by Simulaid and VMD (39,42). The molecular simulation indicates general stability and affinity of both the lead molecules to the binding pockets as predicted from the docking results.

Gene expression studies by quantitative reverse transcription polymerase chain reaction

Total RNA was isolated from FRTL5 cells treated with 1 μM of MS437 for 4 h and untreated control cells using TRIzol reagent (Invitrogen, Life Technologies, Carlsbad, CA) in accordance with the manufacturer's instructions. The RNA purity was evaluated by the ratio of absorbance at

260:280 nm (>1.9). After digestion of genomic DNA by treatment with TURBO DNA-free™ DNase I (Ambion, Austin, TX), total RNA (1 μg) was reverse-transcribed into cDNA with random hexamers using Advantage RT-for-PCR kit (Clontech, Mountain View, CA). The quantitative reverse transcription polymerase chain reactions (qRT-PCRs) were performed using the StepOnePlus Real-time PCR system (Applied Biosystems, Foster City, CA). The reactions were established with 10 μL of SYBR Green master mix (Applied Biosystems), 0.4 μL (2 μM) of sense/antisense gene-specific primers, 2 μL of cDNA, and DEPC-treated water to a final volume of 20 μL. The PCR reaction mix was denatured at 95°C for 60 s before the first PCR cycle. The thermal cycle profile was as follows: denaturizing for 30 s at 95°C, annealing for 30 s at 57–60°C (dependent on primers), and extension for 60 s at 72°C. A total of 40 PCR cycles were used. For each target gene, the relative gene expression was normalized to that of the glyceraldehyde-3-phosphate dehydrogenase (*GAPDH*) housekeeping gene by use of the Applied Biosystem StepOnePlus Real-time PCR systems software. Data presented (mean) are from two independent experiments in which all sample sets were analyzed in triplicate.

Mouse thyroid function testing

Female C57BL/6J mice (Jackson Laboratory) six to eight weeks of age and with a mean body weight of 20–25 g were maintained on a standard diet and received intraperitoneal (i.p.) injections (100 μg/mouse of MS437/MS438) for three consecutive days in a fluid volume of 60–90 μL containing a final concentration of ~25% DMSO. The control animals received diluted vehicle (DMSO) or bovine TSH 30 μg/mouse by the same route. Thyroid hormone (T4) levels were estimated in serum from blood collected by submandibular bleeding prior to treatment (prebleed) and 72 h post-treatment (postbleed). Total T4 was measured by a neonatal T4 RIA kit (Coat-A-Count, Siemens Medical Solutions Diagnostics, Berkeley, CA) according to the manufacturer's protocol. All experiments involving animals were carried out according to the Institutional Animal Care Committee Guidelines.

G protein signaling studies

As outlined before, we developed stable CHO-HA-TSHR cell lines expressing various reporter vectors (CRE-, NFAT-RE, SRE-, and SRF-RE-) for studying the activation of various G proteins. These stable lines were characterized and optimized for responses using positive (TSH, ionomycin, PMA) and negative controls. Prior to measurement of signaling, 20,000 cells were seeded in square-bottom white plates (Nunc cat # 164610) in 20 μL of Ham's F12 complete medium and incubated overnight at 37°C. The complete medium was then replaced with serum free medium for 2 h and then treated with 10 μM of each compound and the appropriate controls for 4 h. At the end of the incubation period, the cells were lysed using 10 μL of Bright-Glo™ reagent and incubated for 2 min at RT, and the plates were read using a BMG Pherastar microplate reader.

PK studies

PK studies were carried out at Sai Life Sciences Ltd. (Pune, India). Briefly, 18 Balb/c mice were used for testing each molecule. The animals were weighed before dose administration and divided into two groups. Group 1 was bolus-dosed intravenously (i.v.), and group II was bolus-dosed via i.p. injection with careful formation of a solution at a dose of 20 mg/kg body weight. Blood samples were collected at predose, and at 2, 4, 6, 12, and 24 h (i.v. and i.p.). Blood was collected from a set of three mice under light isoflurane anesthesia from the retroorbital plexus at each time point in tubes containing K_2EDTA as anticoagulant. Plasma samples were processed for analysis by protein precipitation using acetonitrile. Glipizide was used as internal standard and analyzed by the LC-MS/MS method. PK parameters were calculated using the noncompartmental analysis tool of Phoenix Win Nonlin Enterprise software (v6.3).

Statistical analyses

All curve fitting and EC_{50} calculations were performed using GraphPad Prism v5.02, and statistical differences for *p*-values were calculated using one-way analysis of variance (ANOVA) using Prism.

Results

Identification of positive allosteric modulators of the TSHR

To identify allosteric modulators of the TSHR, we screened 48,224 small molecules from a 100K library using the one-step transcriptional-based bioassay. All compounds were screened at a single concentration of 17 μM in duplicate plates and selected if a significant response was obtained in both plates and with the selection criteria being more than three standard deviations (*SD*) above the baseline activity. The screen of 48,224 molecules resulted in a total of 63 positives, giving a hit ratio of 0.13%. False positives are commonly found in any cell-based signaling assays. Therefore, to identify true agonist compounds, we subjected the most positive 22 of the 63 hits to a second confirmatory testing using TSHR-expressing CHO cells and also CHO cells containing an empty vector (parent cells). Based on this second round of testing, we selected two compounds—MS437 and MS438—as our lead molecules, which showed >10-fold responses above the baseline and no activity on parent CHO luciferase cells. Figure 1A and B shows the structures of these lead molecules, and Figure 1C and D shows the dose–response curves for TSH and lead molecules. Molecule MS437 had an EC_{50} of 13×10^{-8} M, and molecule MS438 had an EC_{50} of 5.3×10^{-8} M.

Specificity of lead molecules

To analyze the specificity of these molecules, the compounds were tested against cells that expressed the LHR or the FSHR. For the LHR cells, we used HEK 293 cells transfected with the rat LH/hCGR, and for FSHR cells, we used primary murine Sertoli cells (line TM4), which express the FSHR and respond to human FSH in a dose-dependent manner. Intracellular cAMP was measured after stimulation with 0.1, 1, and 10 μM of the lead molecules and corresponding positive and negative controls. The two lead molecules failed to show any activity against the LHR or the FSHR-expressing cells, even at the highest concentration used (10 μM); in contrast, they responded to treatment with

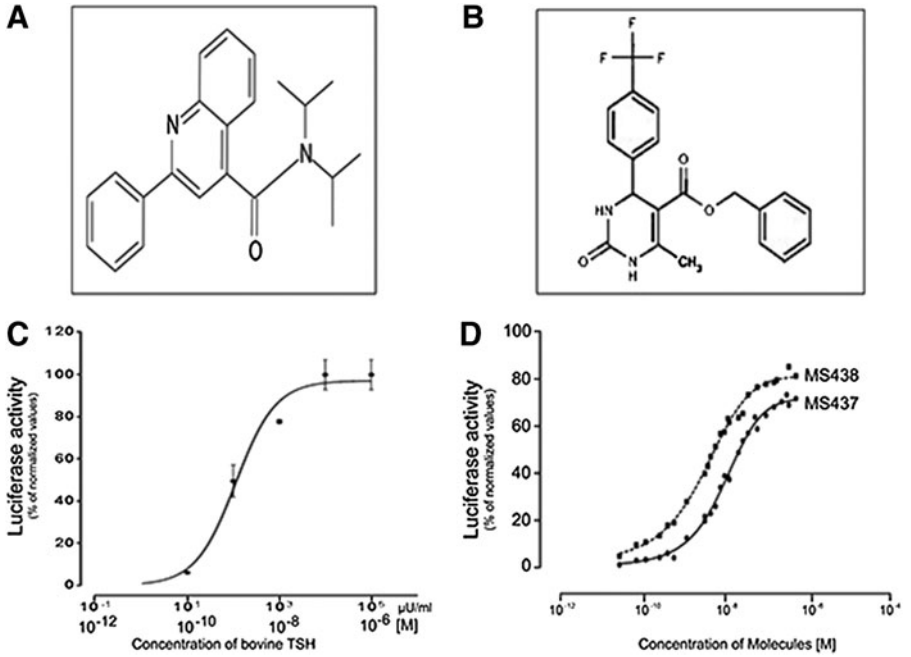

FIG. 1. Structure and potency of selected lead molecules. (**A**) Chemical structure of compound MS437: *N*,*N*-diisopropyl-2-phenyl-4 quinolinecarboxamide. (**B**) Chemical structure of compound MS438: Benzyl 6 methyl-2-oxo-4-[4-(trifluoromethyl) phenyl]-1,2,3,4-tetrahydro-5-pyrimidinecarboxylate. (**C**) Dose–response relationship of bovine thyrotropin (TSH) in CHO cells stably expressing hemagglutinin thyrotropin receptor (HA-TSHR) and pGL4.29 [luc2P/CRE/Hygro]. Luciferase was measured using the substrate Bright-Glo™ and read using an Envision (Perkin Elmer, Inc.) microplate reader. (**D**) CHO cells stably expressing HA-TSHR and pGL4.29 [luc2P/CRE/Hygro] were also exposed to different concentrations of MS437 and MS438. The data in (**C**) and (**D**) were normalized against forskolin. In (**C**), the bolded and italicized *x*-axis scale reflects the concentration of bovine TSH represented in moles. This is a representative graph out of three independent experiments.

their respective ligands hCG (1000 μIU/mL) and human FSH (700 μIU/mL) incorporated as positive controls (Fig. 2).

Defining the binding sites

Small molecules are known to often activate GPCRs in an allosteric manner by binding to the TMD of the receptor (43). To examine if molecules MS437 and MS438 bind to the TMD of the TSHR, we used a chimeric construct as schematically represented in Figure 3A. In this construct, the TSHR ectodomain is replaced with the LHR ectodomain, but it retains the complete TSHR TMD (29). Stable cells co-transfected with this chimeric receptor and a luciferase construct responded to hCG (1000 μIU/mL) but not to recombinant human TSH (3000 μIU/mL) indicating the specificity of the ligand binding ectodomain. On exposure to 10 μM of MS437 and MS438, the cells showed equivalent or greater responses compared to hCG and forskolin (Fig. 3B top and bottom panels), indicating that the molecules bound to the serpentine portion of the TSHR.

To identify the binding pocket(s) of the lead molecules, they were docked to the TM region using a structure of the TSHR TM region developed in our laboratory by homology modeling based on the rhodopsin crystal structure. By docking these molecules using Autodock, we were able to show their putative interaction with residues in the intrahelical region of TM3. As per this docking, molecule MS437 interacts with threonine 501 (T501) of TM3 (Fig. 3D), and molecule MS438 interacts with residues serine 505 (S505) and glutamic acid 506 (E506) respectively (Fig. 3E). A preliminary molecular dynamics simulation of just the TMD and the docked ligand showed no tendency of the ligands to leave their site.

Classical and nonclassical G protein signaling studies

The TSHR has been reported to activate members of all four G protein families ($G_{s\alpha}$, $G_{q/11}$, $G_{\beta\gamma}$, and $G_{12/13}$) (44). We studied the signaling potential of our two lead small molecules using a quantitative technique via the tagged response elements for CRE, SRE, SF-SRE, and NFAT (30). Using these constructs, the major pathway that was activated by MS437 and MS438 was the classical $G_{s\alpha}$ pathway where we saw a robust and significant response similar to TSH as indicated in Figure 4A. Examining the other G proteins for nonclassical pathway responses, we observed that the MS437 and MS438 molecules were able to activate $G_{q/11}$ by increasing NFAT and $G\alpha_{12}$ by stimulating a SRE luciferase reporter (Fig. 4B and C). Neither MS437 nor MS438 showed any significant activation of RhoA kinase via SRF luciferase, indicating that the small molecules did not engage $G_{\beta\gamma}$ (Fig. 4D). The activation of $G_{s\alpha}$ and G_q by the small molecules, similar to TSH, strongly suggests that these molecules could initiate iodine organification and thyroid hormone secretion and promote thyroid growth by their ability to engage in G_q activation in the same manner as TSH itself (45–48).

Thyroid-specific gene expression in thyrocytes

In order to confirm the activity of these molecules on more physiologically relevant cells, we examined thyroid-specific

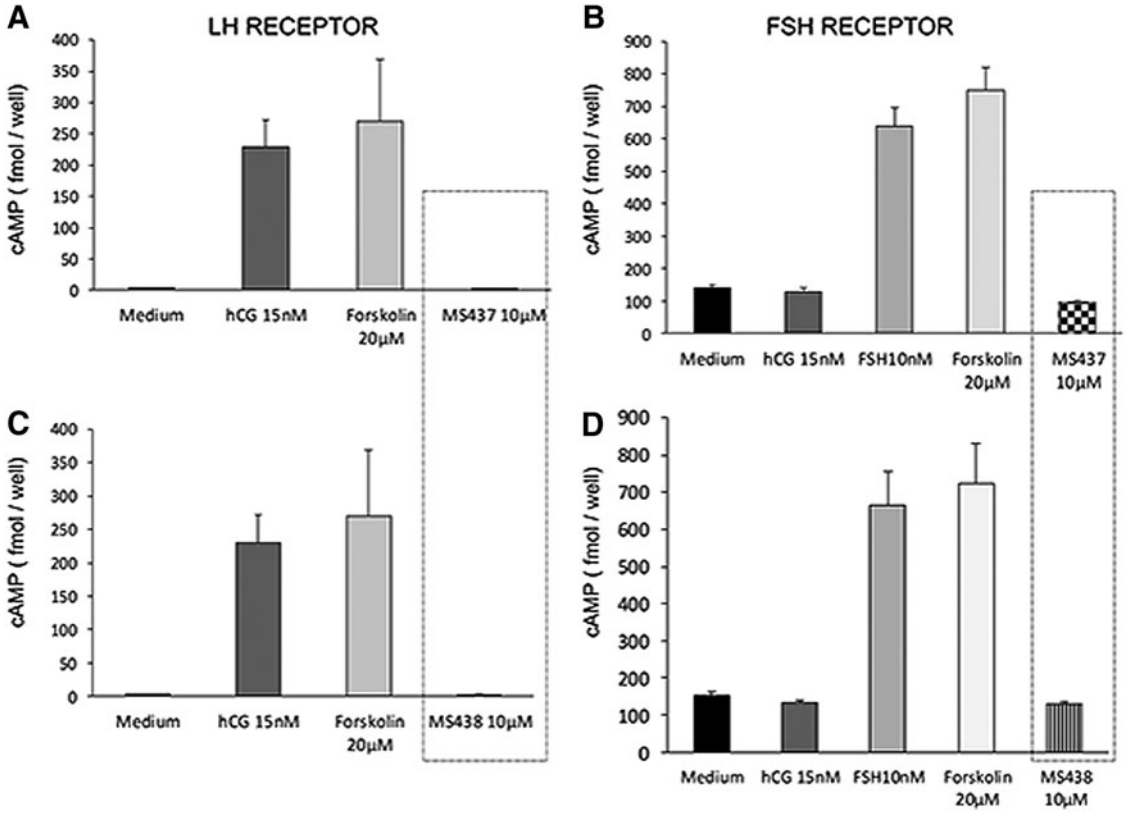

FIG. 2. Specificity of the molecules. (**A**) and (**C**) HEK 293 cells overexpressing the luteinizing hormone/human chorionic gonadotropin receptor (LH/hCGR) were used to test the specificity of MS437 and 439 molecules against the LH/hCGR. As indicated in the boxed area, the two molecules showed no activity on the LH/hCGR-expressing cells up to the highest concentration of 10 μM when assessed by measuring intracellular cAMP generation. The cells show a response to hCG and forskolin as indicated by the gray bars. (**B**) and (**D**) Similarly, to test their specificity against the FSHR, we used a murine Sertoli cell line (TM4), which responds to follicle stimulating hormone (FSH) but not to hCG as indicated. However, molecules MS437 and MS438 did not stimulate a response in these cells, supporting their specificity for the TSHR. These data are representative of two independent experiments.

gene expression using rat thyrocytes (FRTL5). We tested the effects of these two molecules on expression of mRNA of the thyroglobulin (*TG*), sodium-iodide symporter (*NIS*), thyroid peroxidase (*TPO*), and the *TSHR* genes. Prior to exposure, the cells were deprived of TSH for 48 h and starved in serum-free medium for another 2 h. A single-dose treatment of 1 μM of MS437 and MS438 for 4 h showed a two- to eightfold increase in thyroid-specific gene expression (*Tg*, *NIS*, and *TSHR*) when measured by qPCR. These data show that the SMLs had the ability to exert their effects on thyrocytes that express relatively low levels of the TSHR compared to the previously transfected cell lines (Fig. 4E).

In vivo *potency of the lead molecules*

In order to show that these lead molecules are potential candidates to develop clinically relevant drugs, we tested their ability to cause release of thyroid hormones *in vivo*. T4 levels were measured in male C57BL/6J mice after three i.p. bolus injections of 100 μg per mouse per day (total of 0.3 mg per mouse) of MS437 and MS438 dissolved in < 50% DMSO. In this protocol of prolonged treatment, we saw a sustained increase in serum T4 levels (Fig. 5A). This *in vivo* T4 release study clearly indicates the potency of our lead molecules as agonists to the TSHR.

PK studies

The *in vivo* potency studies allowed us to pursue standard PK analyses of the two lead molecules. As described, a single bolus injection of each compound at a dose of 20 mg/kg was given to Balb/c mice (weight 20–35 g each, $\sim$0.4 mg per mouse) by i.v. and i.p. routes, and the murine plasma was analyzed by mass spectrometry at different points after reaching T_{max} (Fig. 5B and C). Although the time course of clearance was similar by both routes of administration, we observed a half-life ($T_{1/2}$) of 3 h for MS437 compared to a shorter half-life ($T_{1/2}$) of 1 h for MS438 when measuring the half-life of the lead molecules. However, the $T_{1/2}$ for both routes of administration remain the same, as $T_{1/2}$ is calculated from the terminal elimination points. Both compounds show moderate plasma clearance (MS437 = 24.13 mL/min/kg and MS438 = 29.63 mL/min/kg), high volume of distribution (MS437 = 9.6-fold higher vs. MS438 = 4.6-fold higher than total body water) indicating extravascular distribution. In particular, compound MS437 fits into a good PK parameter category with high exposure after i.p. administration.

Discussion

HTS approaches play a central role in identifying small molecules that have intrinsic activity (49), and this approach

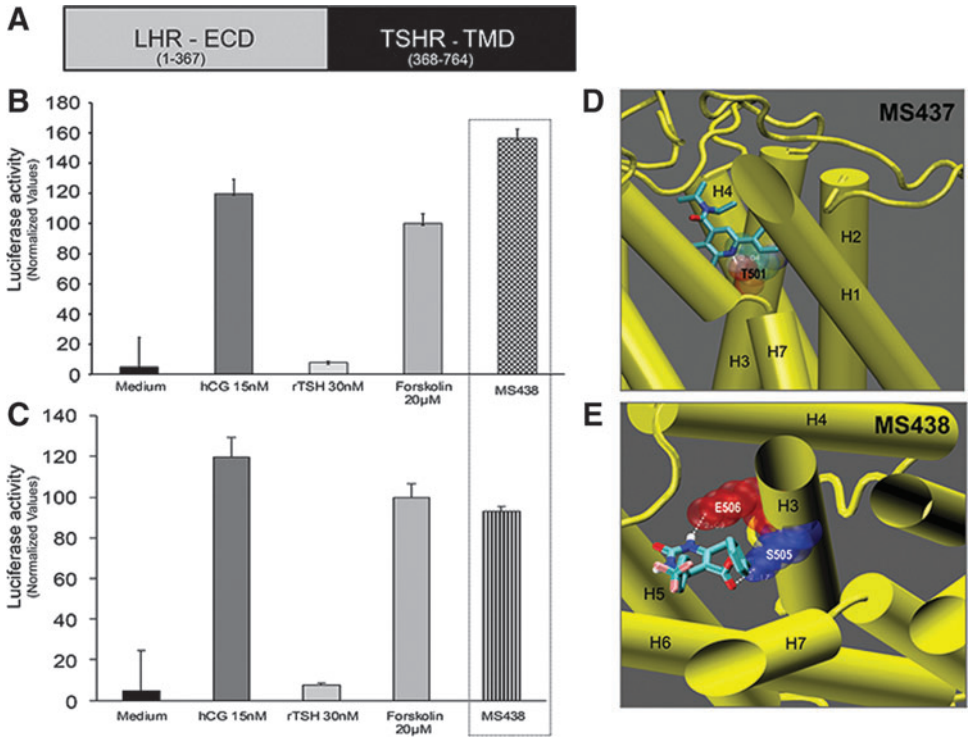

FIG. 3. Allosteric activation of the TSHR. (**A**) Schematic diagram of the chimeric receptor used to ascertain allosteric activation by the two lead molecules. In this construct, the large ectodomain of the TSHR was exchanged for the LHR ectodomain but retains the transmembrane domain (TMD) of the TSHR (black region) (29). (**B**) and (**C**) When cells stably expressing the chimeric receptor and the pGL4.29 [luc2P/ CRE/Hygro] luciferase vector were treated with the TSHR agonist molecules (hatched bars), they showed robust responses. The functionality of the cells is indicated by their specific response to hCG. (**D**) and (**E**) Docking of the molecules into the homology model of the TSHR showed the intrahelical binding of MS437 and MS438 to TMH3. (**D**) shows that molecule MS437 makes a single hydrogen bond with threonine 501 (T501) of TMH3 and Panel E shows that MS438 has two contacts points making hydrogen bonds with serine 505 (S505) and glutamic acid 506 (E506) of TMH3 in the TMD.

has been used to identify molecules targeting the TSHR. However, the first reported agonists to the TSHR were identified based on chemical modification of thienopyrimidine org41841, which was previously identified as an agonist to the LH/hCGR (18,50). Subsequent successful agonists and antagonists to the TSHR reported by Neumann *et al*. (51) have been obtained by a combination of HTS and meticulous chemical modifications. The reported agonist compound 2 (52) stimulated thyroid-specific gene expression in primary human thyrocytes and produced thyroid hormone in mice after administration of 0.5 mg of the molecule. We ventured to identify additional small molecule candidates against the TSHR with the intention of developing greater or unique activities. In this report, we describe the identification and characterization of two novel small molecule agonists detected using a new high-throughput assay.

Our high-throughput strategy employed a remarkably sensitive and precise one-step transcriptional-based assay for measuring interaction of TSH or small molecules with the TSHR. In this system, cAMP responses modulated by the binding of TSH or small molecules were detected as luciferase generation in transfected heterologous co-expressing the TSHR and a CRE-luciferase construct. Initial optimization and validation of the assay gave robust Z′ scores (Z′ = 0.6–0.8), Z′ being a parameter for the measurement of the robustness of a high-throughput assay (32). Using a 384-well format, we screened 48,224 compounds, and found 63 molecules that showed activation of the TSHR. These ''hits'' were further refined and resulted in the selection of two molecules showing consistent and vigorous dose–response relationships with an EC_{50} in the nanomolar range similar to the previous report (15) and approximately equipotent to bovine TSH. Furthermore, these molecules had structures that were dissimilar to any TSHR agonists reported so far (15) (Fig. 1). We refer to these two lead agonist molecules as MS437 and MS438.

Having shown no interaction with the parent control cells (CHO luciferase), which express a variety of receptors including adrenergic receptors, our next approach was to test the specificity of the lead molecules by examining their interaction with the LH/hCGR and the FSHR. The two lead molecules, even at 10 μM (10^{-5} M) concentrations, caused no response with cells expressing the LH/hCGR or cells expressing the FSHR (Fig. 2) as found previously (15). This is in contrast to an earlier TSHR agonist active in nanomolar concentrations but which had clear specificity spillover (19). Although the lead molecules did not interact with the receptors tested, including the many receptors expressed on control CHO cells, the GPCR family of receptors is large, and we cannot exclude any interactions at this time. Thus, our two lead molecules—MS437 and MS438—appear to have selectivity and potency for the TSHR and have efficacy equivalent to TSH in cells expressing the TSHR.

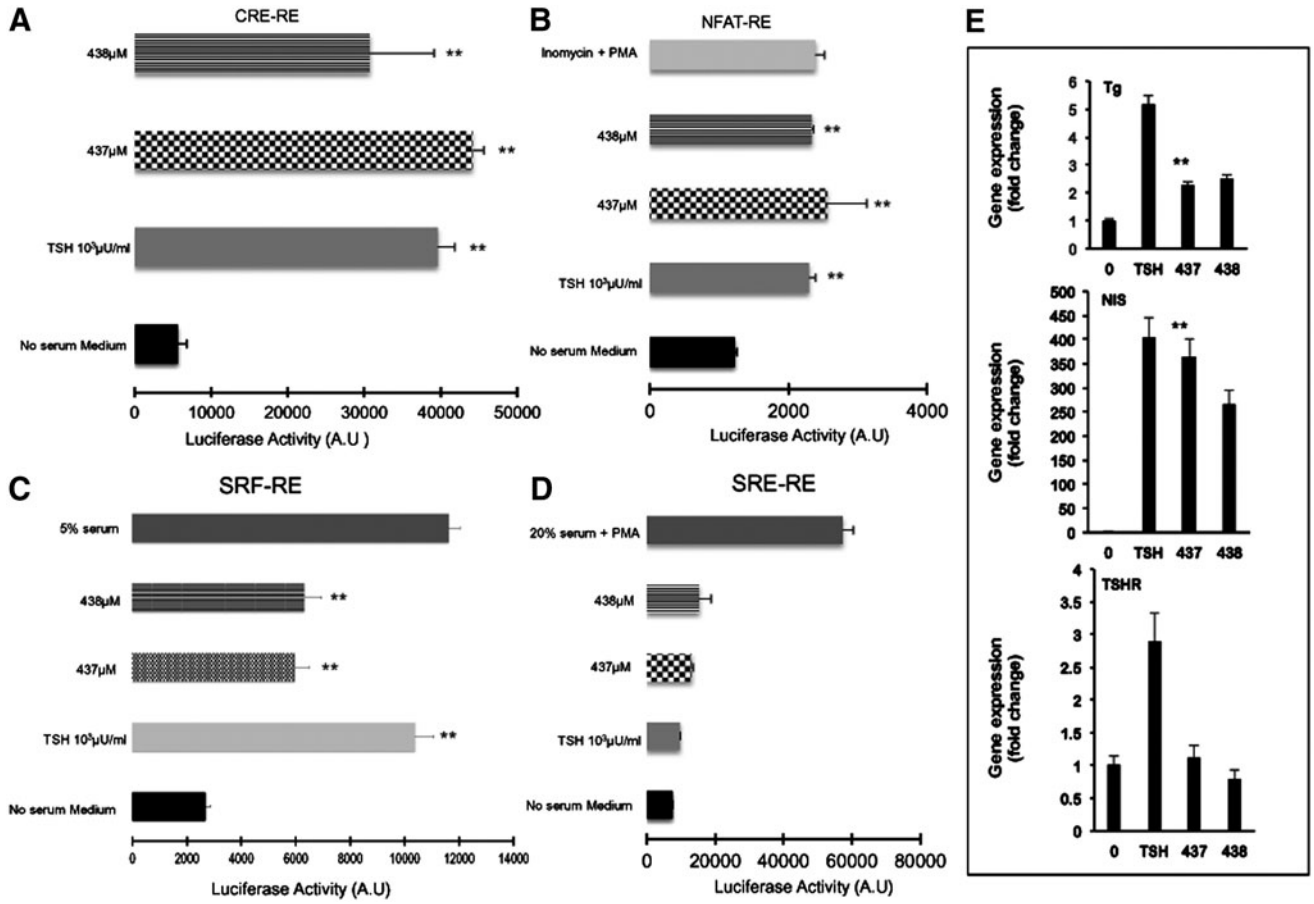

FIG. 4. TSHR signaling via different G proteins. In order to study the engagement of different G proteins with the TSHR, we generated stable CHO cells containing various luciferase reporter constructs with distinct response elements as detailed in Materials and Methods. (**A**) Upon stimulation of the TSHR, the most predominant activation occurred through $G_{s\alpha}$, which lead to an increase in cAMP via activation of adenylyl cyclase. The cAMP increase ultimately results in the activation of the CRE fused to the *luciferase* gene. As shown, molecules MS437 and MS438 were potent stimulators of cAMP generation via activation of $G_{s\alpha}$ (**$p < 0.001$). (**B**) Similarly, a stable line of CHO cells co-transfected with the TSHR and an NFAT response element-containing luciferase construct in order to measure signaling through $G_{\alpha q}$ showed that the two lead molecules were capable of activating this G protein to the same extent as 1000 μIU/mL of TSH or, as control, 1 μM ionomycin + 10 ng/mL Phorbal-12-myristate-13-actate (PMA; **$p < 0.01$). (**C**) SRF-RE is a response element fused to the *luciferase* reporter gene and is able to measure $G_{\alpha 12}$ activation via enhancement of the second messenger Rho A kinase. The data indicate that the molecules are able to engage this pathway as was both 20% serum and TSH, which acted as positive controls (**$p < 0.01$). (**D**) Activation of $G_{\beta\gamma}$ leads to activation of second messenger $ERK_{1/2}$, which in turn can activate the SRE-RE. This graph shows that the cells are responsive to 20% serum with 10 ng/mL of Phorbol-12-myristate-13-acetate (PMA) as a positive control. No responses were seen with TSH or MS437 and MS438 (**$p < 0.01$). (**E**) Rat thyrocytes (FRTL5) grown to near confluence in 6H medium were maintained for another 48 h without TSH. Prior to RNA extraction, the cells were treated with TSH 1000 μIU/mL or 10 μM of MS437 at 37°C for 4 h. The different panels indicate the fold changes in the expression of mRNA for *Tg* (top panel), *NIS* (middle panel), and the *TSHR* (lower panel) in the presence of medium only, TSH, or molecule MS437. Small molecule MS437 increased the expression anywhere between two- and sixfold for each of the genes assayed (**$p < 0.01$).

Small molecule agonists and antagonists, unlike TSH, have been shown to mediate their signaling effects by binding to the TMD of the TSHR (20). This allosteric mode of action may result from the inherent property of small molecules, including their small size and hydrophobic nature. However, it has been shown that the TSHR contains clusters of residues with allosteric potential encompassing signaling-sensitive amino acids within the helices of the TMD (21). To determine if our lead molecules were allosteric modulators, as expected, we tested their receptor-stimulating activity on a chimeric receptor in which the major part of its ectodomain consists of the LHR sequence fused to the native human TSHR TMD. The two lead molecules activated luciferase generation with this chimeric receptor expressed in parental CHO cells but were unable to activate the native LH/hCGR as described earlier. Hence, the molecules required the TSHR TMD in order to signal, showing that they bind to the serpentine domain of the receptor. This is in great contrast to TSH, which exerts its effect by binding mainly to epitopes in the LRD of the ectodomain but also has other binding sites in the large extracellular domain and extracellular loops (53,54).

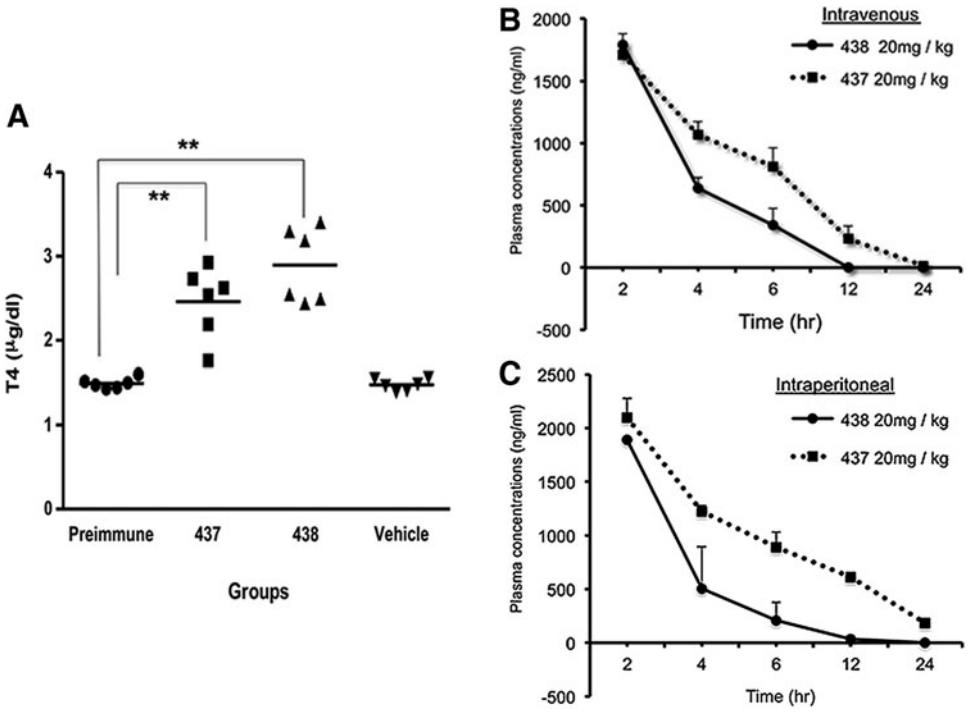

FIG. 5. Small molecule-induced T4 secretion and pharmacokinetics. (**A**) Male mice (C57BL/6J; $n=2$ per group) were subjected to intraperitoneal (i.p.) injection of MS437 and MS438 with a single dose of 100 μg per mouse per day using the small molecules emulsified in $<50\%$ DMSO and compared with vehicle alone–injected mice for three consecutive days. This figure illustrates the distribution of the individual readings of each mouse from the samples collected after 72 h. The mean of the distribution is indicated by the horizontal bar. When compared to the pre-immune and vehicle-injected controls, both MS437 and MS438 induced an increase in serum total thyroxine (T4) levels after 72 h of treatment ($^{**}p<0.01$). (**B**) and (**C**) Male mice (Balb/c; $n=18$ per group) were dosed intravenously (i.v.; group I) or i.p. (group II) at 20 mg/kg of body weight. The compounds were prepared in formulation containing DMSO, propylene glycol of Cremphor EL, PEG400, and saline. The dosing volume administered for the i.v. route was 5 mL/kg, and for the i.p. route was 10 mL/kg. Blood samples were collected from three mice at the start and then at each time point of 2, 4, 6, 12, and 24 h (both i.v. and i.p.). The samples were analyzed by mass spectrometry with internal standards. As the $T_{1/2}$ is calculated from terminal elimination points, it remains the same for both routes of compound injection. Molecule MS437 had a longer serum half-life (3.10 h) compared to MS438 (1.02 h). The difference in strain of mice used for the pharmokinetic study and the T4 release study is based on availability of animals at the time.

To substantiate our *in vitro* findings and to map the binding sites of these molecules, we used a new homology model of the TSHR TMD with its loop structures. These docking studies predicted that both molecules bind to the intrahelical region of the transmembrane helix 3 (TMH3) and result in hydrogen bonding with residues T502 for MS437 and E505 and E506 for MS438 of TMH3 (Fig. 3); this contrasts with the binding of an earlier reported agonist to TMH5 (15). Preliminary molecular dynamic simulation studies carried out for 10 ns showed that binding of these molecules to TMH3 was of high affinity, allowing them to be retained in their binding pocket.

The potential of a small molecule as a drug candidate lies primarily in the selective activation or inhibition of the receptor. Although it has been shown that the TSHR is capable of engaging multiple G proteins (55), recent studies from our laboratory using different autoantibodies to the TSHR (56) have shown that engaging different epitopes of the receptor can result in a cascade of differential signaling via classical (cAMP-PKA) and nonclassical (MAPK/Rho) signaling pathways (47,57). Furthermore, such signaling may alter the immunopathology of autoimmune thyroid disease (58). Using a luciferase reporter that was transcriptionally activated by a cascade of downstream messengers induced by different G proteins, we studied $G_{s\alpha}$, $G_{\alpha q}$, $G_{\beta\gamma}$, and $G_{\alpha 12}$ activation by the lead small molecules. Like TSH, the two lead agonists primarily engaged $G_{s\alpha}$, $G_{\alpha q}$, and $G_{\alpha 12}$, resulting in endogenous gene expression of the *Tg*, *NIS*, and the *TSHR* genes (Fig. 4A–D).

To be potential drug candidates, the small molecules need to display *in vivo* activity, and we show their ability to stimulate the thyroid gland and increase secretion of T4 in mice. The PK studies indicate that both lead molecules have good PK parameters with moderate plasma clearance and half-life, and both are capable of enhancing thyroid hormone secretion. Furthermore, *in vitro* cytotoxic studies showed no cytotoxic effects at the highest working concentrations (data not shown) of these two molecules. Hence, the data show that we have identified two structurally unique lead molecules that are selective allosteric agonists to the TSHR. The molecular scaffolds of these two lead molecules hold promise for chemical optimization and molecular changes to derive even more potent agonists and antagonists to the TSHR.

Acknowledgments

The authors thank Dr. Yaron Tomer and Dr. Mone Zaidi from the Department of Medicine, Icahn School of Medicine at Mount Sinai, for their helpful discussions. We are also thankful to Dr. R. Baliram and Dr. X.Yin for their contributions. The luciferase constructs mentioned in this study were a gift from Dr. Frank Fan, Director of Research, at Promega Corp. We also thank the computational resources and staff expertise provided by the Department of Scientific Computing at Icahn School of Medicine at Mount Sinai, New York.

This work was supported in part by NIH grants DK069713, DK052464, and the VA Merit Award program (to T.F.D.).

Author Disclosure Statement

No competing financial interests exist.

References

1. Ladenson PW, Braverman LE, Mazzaferri EL, Brucker-Davis F, Cooper DS, Garber JR, Wondisford FE, Davies TF, DeGroot LJ, Daniels GH, Ross DS, Weintraub BD 1997 Comparison of administration of recombinant human thyrotropin with withdrawal of thyroid hormone for radioactive iodine scanning in patients with thyroid carcinoma. N Engl J Med **337:**888–896.
2. Mazzaferri EL, Kloos RT 2002 Is diagnostic iodine-131 scanning with recombinant human TSH useful in the follow-up of differentiated thyroid cancer after thyroid ablation? J Clin Endocrinol Metab **87:**1490–1498.
3. Sanders J, Chirgadze DY, Sanders P, Baker S, Sullivan A, Bhardwaja A, Bolton J, Reeve M, Nakatake N, Evans M, Richards T, Powell M, Miguel RN, Blundell TL, Furmaniak J, Smith BR 2007 Crystal structure of the TSH receptor in complex with a thyroid-stimulating autoantibody. Thyroid **17:**395–410.
4. Chen CR, Salazar LM, McLachlan SM, Rapoport B 2012 The thyrotropin receptor hinge region as a surrogate ligand: identification of loci contributing to the coupling of thyrotropin binding and receptor activation. Endocrinology **153:**5058–5067.
5. Krause G, Kreuchwig A, Kleinau G 2012 Extended and structurally supported insights into extracellular hormone binding, signal transduction and organization of the thyrotropin receptor. PLoS One 7:e52920.
6. Mizutori Y, Chen CR, McLachlan SM, Rapoport B 2008 The thyrotropin receptor hinge region is not simply a scaffold for the leucine-rich domain but contributes to ligand binding and signal transduction. Mol Endocrinol **22:**1171–1182.
7. Jiang X, Liu H, Chen X, Chen PH, Fischer D, Sriraman V, Yu HN, Arkinstall S, He X 2012 Structure of follicle-stimulating hormone in complex with the entire ectodomain of its receptor. Proc Natl Acad Sci U S A **109:**12491–12496.
8. Davies TF, Ando T, Lin RY, Tomer Y, Latif R 2005 Thyrotropin receptor-associated diseases: from adenomata to Graves' disease. J Clin Invest **115:**1972–1983.
9. Davies T, Marians R, Latif R 2002 The TSH receptor reveals itself. J Clin Invest **110:**161–164.
10. Smith BR, Hall R 1974 Thyroid-stimulating immunoglobulins in Graves' disease. Lancet **2:**427–431.
11. Abe E, Marians RC, Yu W, Wu XB, Ando T, Li Y, Iqbal J, Eldeiry L, Rajendren G, Blair HC, Davies TF, Zaidi M 2003 TSH is a negative regulator of skeletal remodeling. Cell **115:**151–162.
12. Bahn RS 2004 TSH receptor expression in orbital tissue and its role in the pathogenesis of Graves' ophthalmopathy. J Endocrinol Invest **27:**216–220.
13. Elgadi A, Zemack H, Marcus C, Norgren S 2010 Tissue-specific knockout of TSHr in white adipose tissue increases adipocyte size and decreases TSH-induced lipolysis. Biochem Biophys Res Commun **393:**526–530.
14. Sanders J, Miguel RN, Furmaniak J, Smith BR 2010 TSH receptor monoclonal antibodies with agonist, antagonist, and inverse agonist activities. Methods Enzymol **485:**393–420.
15. Neumann S, Huang W, Titus S, Krause G, Kleinau G, Alberobello AT, Zheng W, Southall NT, Inglese J, Austin CP, Celi FS, Gavrilova O, Thomas CJ, Raaka BM, Gershengorn MC 2009 Small-molecule agonists for the thyrotropin receptor stimulate thyroid function in human thyrocytes and mice. Proc Natl Acad Sci U S A **106:**12471–12476.
16. Neumann S, Nir EA, Eliseeva E, Huang W, Marugan J, Xiao J, Dulcey AE, Gershengorn MC 2014 A Selective TSH receptor antagonist inhibits stimulation of thyroid function in female mice. Endocrinology **155:**310–314.
17. Neumann S, Pope A, Geras-Raaka E, Raaka BM, Bahn RS, Gershengorn MC 2012 A drug-like antagonist inhibits thyrotropin receptor-mediated stimulation of cAMP production in Graves' orbital fibroblasts. Thyroid **22:**839–843.
18. Jaschke H, Neumann S, Moore S, Thomas CJ, Colson AO, Costanzi S, Kleinau G, Jiang JK, Paschke R, Raaka BM, Krause G, Gershengorn MC 2006 A low molecular weight agonist signals by binding to the transmembrane domain of thyroid-stimulating hormone receptor (TSHR) and luteinizing hormone/chorionic gonadotropin receptor (LHCGR). J Biol Chem **281:**9841–9844.
19. van Koppen CJ, de Gooyer ME, Karstens WJ, Plate R, Conti PG, van Achterberg TA, van Amstel MG, Brands JH, Wat J, Berg RJ, Lane JR, Miltenburg AM, Timmers CM 2012 Mechanism of action of a nanomolar potent, allosteric antagonist of the thyroid-stimulating hormone receptor. Br J Pharmacol **165:**2314–2324.
20. Hoyer I, Haas AK, Kreuchwig A, Schulein R, Krause G 2013 Molecular sampling of the allosteric binding pocket of the TSH receptor provides discriminative pharmacophores for antagonist and agonists. Biochem Soc Trans **41:**213–217.
21. Kleinau G, Haas AK, Neumann S, Worth CL, Hoyer I, Furkert J, Rutz C, Gershengorn MC, Schulein R, Krause G 2010 Signaling-sensitive amino acids surround the allosteric ligand binding site of the thyrotropin receptor. FASEB J **24:**2347–2354.
22. Kleinau G, Hoyer I, Kreuchwig A, Haas AK, Rutz C, Furkert J, Worth CL, Krause G, Schulein R 2011 From molecular details of the interplay between transmembrane helices of the thyrotropin receptor to general aspects of signal transduction in family a G-protein-coupled receptors (GPCRs). J Biol Chem **286:**25859–25871.
23. Haas AK, Kleinau G, Hoyer I, Neumann S, Furkert J, Rutz C, Schulein R, Gershengorn MC, Krause G 2011 Mutations that silence constitutive signaling activity in the allosteric ligand-binding site of the thyrotropin receptor. Cell Mol Life Sci **68:**159–167.
24. Kleinau G, Neumann S, Gruters A, Krude H, Biebermann H 2013 Novel insights on thyroid-stimulating hormone receptor signal transduction. Endocr Rev **34:**691–724.

25. Audet M, Bouvier M 2012 Restructuring G-protein-coupled receptor activation. Cell **151:**14–23.
26. Govaerts C, Lefort A, Costagliola S, Wodak SJ, Ballesteros JA, Van Sande J, Pardo L, Vassart G 2001 A conserved Asn in transmembrane helix 7 is an on/off switch in the activation of the thyrotropin receptor. J Biol Chem **276:**22991–22999.
27. Davies TF, Ali MR, Latif R 2014 Allosteric modulators hit the TSH receptor. Endocrinology **155:**1–5.
28. Latif R, Ando T, Davies TF 2004 Monomerization as a prerequisite for intramolecular cleavage and shedding of the thyrotropin receptor. Endocrinology **145:**5580–5588.
29. Nagayama Y, Wadsworth HL, Chazenbalk GD, Russo D, Seto P, Rapoport B 1991 Thyrotropin-luteinizing hormone/chorionic gonadotropin receptor extracellular domain chimeras as probes for thyrotropin receptor function. Proc Natl Acad Sci U S A **88:**902–905.
30. Cheng Z, Garvin D, Paguio A, Stecha P, Wood K, Fan F 2010 Luciferase reporter assay system for deciphering GPCR pathways. Curr Chem Genomics **4:**84–91.
31. Fan F, Wood KV 2007 Bioluminescent assays for high-throughput screening. Assay Drug Dev Technol **5:**127–136.
32. Zhang JH, Chung TD, Oldenburg KR 1999 A simple statistical parameter for use in evaluation and validation of high throughput screening assays. J Biomol Screen **4:**67–73.
33. Palczewski K, Kumasaka T, Hori T, Behnke CA, Motoshima H, Fox BA, Le Trong I, Teller DC, Okada T, Stenkamp RE, Yamamoto M, Miyano M 2000 Crystal structure of rhodopsin: a G protein-coupled receptor. Science **289:**739–745.
34. Ali MR, Latif R, Davies TF, Mezei M 2014 Monte Carlo loop refinement and virtual screening of the thyroid-stimulating hormone receptor transmembrane domain. J Biomol Struct Dyn 2014 Jul 11:1–13. [Epub ahead of print]
35. Cui M, Mezei M, Osman R 2008 Prediction of protein loop structures using a local move Monte Carlo approach and a grid-based force field. Protein Eng Des Sel **21:**729–735.
36. Frisch MJ, Trucks GW, Schlegel HB, Scuseria GE, Robb MA, Cheeseman JR, Scalmani G, Barone V, Mennucci B, Petersson GA, Nakatsuji H, Caricato M, Li X, Hratchian HP, Izmaylov AF, Bloino J, Zheng G, Sonnenberg JL, Hada M, Ehara M, Toyota K, Fukuda R, Hasegawa J, Ishida M, Nakajima T, Honda Y, Kitao O, Nakai H, Vreven T, Montgomery JA, Peralta JE, Ogliaro F, Bearpark M, Heyd JJ, Brothers E, Kudin KN, Staroverov VN, Kobayashi R, Normand J, Raghavachari K, Rendell A, Burant JC, Iyengar SS, Tomasi J, Cossi M, Rega N, Millam JM, Klene M, Knox JE, Cross JB, Bakken V, Adamo C, Jaramillo J, Gomperts R, Stratmann RE, Yazyev O, Austin AJ, Cammi R, Pomelli C, Ochterski JW, Martin RL, Morokuma K, Zakrzewski VG, Voth GA, Salvador P, Dannenberg JJ, Dapprich S, Daniels AD, Farkas, Foresman JB, Ortiz JV, Cioslowski J, Fox DJ 2009 Gaussian 09, Revision B.01, Wallingford CT.
37. Wang J, Wang W, Kollman PA, Case DA 2006 Automatic atom type and bond type perception in molecular mechanical calculations. J Mol Graph Model **25:**247–260.
38. Wang J, Wolf RM, Caldwell JW, Kollman PA, Case DA 2004 Development and testing of a general amber force field. J Comput Chem **25:**1157–1174.
39. Mezei M 2010 Simulaid: a simulation facilitator and analysis program. J Comput Chem **31:**2658–2668.
40. Mezei M, Zhou MM 2010 Dockres: a computer program that analyzes the output of virtual screening of small molecules. Source Code Biol Med **5:**2.
41. Case DA, Darden TA, Cheatham TE, Simmerling CL, Wang J, Duke RE, Luo R, Walker RC, Zhang W, Merz KM, Roberts B, Hayik S, Roitberg A, Seabra G, Swails J, Goetz AW, Kolossváry I, Wong KF, Paesani F, Vanicek J, Wolf RM, Liu J, Wu X, Brozell SR, Steinbrecher T, Gohlke H, Cai Q, Ye X, Hsieh MJ, Cui G, Roe DR, Mathews DH, Seetin MG, Salomon-Ferrer R, Sagui C, Babin V, Luchko T, Gusarov S, Kovalenko A, Kollman PA 2012 AMBER 12. University of California, San Francisco.
42. Humphrey W, Dalke A, Schulten K 1996 VMD: visual molecular dynamics. J Mol Graph **14:**33–38, 27–38.
43. Leach K, Sexton PM, Christopoulos A 2007 Allosteric GPCR modulators: taking advantage of permissive receptor pharmacology. Trends Pharmacol Sci **28:**382–389.
44. Duprez L, Parma J, Van Sande J, Rodien P, Dumont JE, Vassart G, Abramowicz M 1998 TSH Receptor Mutations and Thyroid Disease. Trends Endocrinol Metab **9:**133–140.
45. Postiglione MP, Parlato R, Rodriguez-Mallon A, Rosica A, Mithbaokar P, Maresca M, Marians RC, Davies TF, Zannini MS, De Felice M, Di Lauro R 2002 Role of the thyroid-stimulating hormone receptor signaling in development and differentiation of the thyroid gland. Proc Natl Acad Sci U S A **99:**15462–15467.
46. Rapoport B, Chazenbalk GD, Jaume JC, McLachlan SM 1998 The thyrotropin (TSH) receptor: interaction with TSH and autoantibodies. Endocr Rev **19:**673–716.
47. Morshed SA, Latif R, Davies TF 2009 Characterization of thyrotropin receptor antibody-induced signaling cascades. Endocrinology **150:**519–529.
48. Kero J, Ahmed K, Wettschureck N, Tunaru S, Wintermantel T, Greiner E, Schutz G, Offermanns S 2007 Thyrocyte-specific Gq/G11 deficiency impairs thyroid function and prevents goiter development. J Clin Invest **117:**2399–2407.
49. Inglese J, Johnson RL, Simeonov A, Xia M, Zheng W, Austin CP, Auld DS 2007 High-throughput screening assays for the identification of chemical probes. Nat Chem Biol **3:**466–479.
50. Moore S, Jaeschke H, Kleinau G, Neumann S, Costanzi S, Jiang JK, Childress J, Raaka BM, Colson A, Paschke R, Krause G, Thomas CJ, Gershengorn MC 2006 Evaluation of small-molecule modulators of the luteinizing hormone/choriogonadotropin and thyroid stimulating hormone receptors: structure–activity relationships and selective binding patterns. J Med Chem **49:**3888–3896.
51. Gershengorn MC, Neumann S 2012 Update in TSH receptor agonists and antagonists. J Clin Endocrinol Metab **97:**4287–4292.
52. Neumann S, Gershengorn MC 2011 Small molecule TSHR agonists and antagonists. Ann Endocrinol (Paris) **72:**74–76.
53. Jeffreys J, Depraetere H, Sanders J, Oda Y, Evans M, Kiddie A, Richards T, Furmaniak J, Rees Smith B 2002 Characterization of the thyrotropin binding pocket. Thyroid **12:**1051–1061.
54. Mueller S, Kleinau G, Jaeschke H, Paschke R, Krause G 2008 Extended hormone binding site of the human thyroid stimulating hormone receptor: distinctive acidic residues in the hinge region are involved in bovine thyroid stimulating hormone binding and receptor activation. J Biol Chem **283:**18048–18055.
55. Allgeier A, Offermanns S, Van Sande J, Spicher K, Schultz G, Dumont JE 1994 The human thyrotropin receptor activates G-proteins Gs and Gq/11. J Biol Chem **269:**13733–13735.
56. Latif R, Teixeira A, Michalek K, Ali MR, Schlesinger M, Baliram R, Morshed SA, Davies TF 2012 Antibody protection

reveals extended epitopes on the human TSH receptor. PLoS One **7:**e44669.
57. Morshed SA, Ando T, Latif R, Davies TF 2010 Neutral antibodies to the TSH receptor are present in Graves' disease and regulate selective signaling cascades. Endocrinology **151:**5537–5549.
58. Morshed SA, Ma R, Latif R, Davies TF 2013 How one TSH receptor antibody induces thyrocyte proliferation while another induces apoptosis. J Autoimmun **47:**17–24.

Address correspondence to:
Rauf Latif, PhD
James J. Peters VAMC
Room 2F-30
130 West Kingsbridge Road
New York, NY 10468

E-mail: rauf.latif@mssm.edu